KSCE Journal of Civil Engineering (2017) 21(7):2707-2716

DOI 10.1007/s12205-017-0435-y

Structural Engineering

pISSN 1226-7988, eISSN 1976-3808
www.springer.com/12205

Seismic Performance of a Four-story Two-bay High-performance Concrete Frame under Low Reversed Cyclic Loading

Weichen Xue* and Xiang Hu**

Received June 3, 2015/Accepted December 4, 2016/Published Online March 7, 2017

Abstract

The purpose of this work is to investigate the seismic performance of a four-story two-bay high-performance concrete (HPC) frame. Low reversed cyclic loading was conducted on a 1/5-scaled HPC frame. Seismic performance of the frame specimen was evaluated in terms of failure pattern, failure mechanism, deformation restoring capacity, displacement ductility and energy dissipation capacity. Test results showed that the specimen failed in the designed failure mechanism, and behaved in a ductile manner and larger energy dissipation capacity. The roof lateral displacement ductility coefficient was 5.69, and the 1st, 2nd, 3rd and 4th inter-story lateral displacement ductility coefficients were 7.95, 7.32, 5.06 and 4.69, respectively. An alternative design principle of frame structures is proposed in this paper to ensure that the beam sidesway mechanism occurs. Parametric analysis of ten frames with different developmental sequence of plastic hinges is conducted by a Finite Element Analysis (FEA) software framework OpenSees. The analytical results showed that the ductility supply of the frame designed according to the proposed design principle was maximized.

Keywords: *high-performance concrete, four-story two-bay frame, seismic performance, low reversed cyclic loading, failure mechanism, design principle*

1. Introduction

High-Performance Concrete (HPC) is a kind of concrete with good durability and work ability, such as toughness, volume stability and low permeability, etc. Note that, in order to obtain the performance, a variety of admixtures, including fly ash, grinded slags and fibers, etc, should be contained in the ingredients of HPC (Neville and Aitcin, 1998). It makes that HPC has to be manufactured and placed much more carefully, and the cost of HPC is a little high.

HPC is often said to be developed based on High-strength Concrete (HSC), but indeed it is not equivalent to HSC (Neville, 1998; Breitenbücher, 1998). For HSC, the increased compressive strength is primarily used, and the cubic compressive strength always required higher than 60 MPa. The efficiency of HPC, however, is not limited to this property but mainly focused on the durability and workability, which lead to construction elements with high economic efficiency, high utility and long-term engineering economy. The use of HPC has become widespread in many major projects, such as 311 South Wacker Drive (USA, 1990), Oriental Pearl Television Tower (China, 1992), Tsing Ma Bridge (China, 1997), Petronas Tower (Malaysia, 1998), Jinmao Building (China, 1999), Shanghai Financial Center (China, 2008) and Shanghai Tower (China, 2015).

The monotonic static behavior of HPC members has been the subject of numerous studies (Lin and Lee, 2001; Prasad *et al*., 2005; Awati and Khadiranaikar, 2012; Biolzi *et al*., 2014). However, experimental studies on seismic performance of HPC structures are few; current investigations are mainly focused on High-strength Concrete (HSC) structural members, including beams, columns and frame joints. The test results of HSC beams under cyclic loads showed that both high and normal strength concrete beams developed ductile flexural responses, and the HSC beams exhibited increased capacity (Fang *et al.*, 1994; Xiao and Ma, 1998). Studies on seismic performance of HSC columns showed that HSC columns and Normal Concrete (NC) columns had similar ductility subjected to the same level of axial load, and curvature ductility of HSC column sections might be greatly improved by configuration of stirrups (Priestley *et al*., 1994; Xiao and Martirossyan, 1998; Woods *et al.,* 2007). The investigations of frame joints concluded that properly designed HSC joints had similar displacement ductility and hysteresis characteristics to NC joints (Alameddine and Ehsani, 1991; Anderson *et al*., 1997; Ashitiani *et al.,* 2014).

The research panel of Tongji University in China has carried out a research program on material and structural behaviors of HPC since 2000 due to the available studies on seismic performance of HPC structures are few. The workability and durability

*Professor, Dept. of Structural Engineering, Tongji University, Shanghai 200092, P. R. China (E-mail: xuewc@tongji.edu.cn)
**Ph.D. Candidate, Dept. of Structural Engineering, Tongji University, Shanghai 200092, P. R. China (Corresponding Author, E-mail: hu_xiang@tongji.edu.cn)

properties of HPC were firstly investigated based on the test results (Wu *et al.,* 2001; Yao *et al.*, 2003). Subsequently, analytical and experimental studies on prestressed and non-prestressed HPC beams and normal Reinforcement Concrete (RC) beams were conducted (Xue, 2008), and the seismic performance of HPC elements and normal RC elements are compared. It shows that the ductility and deformability of HPC elements is better than that of normal RC elements. In addition, two-story two-bay HPC frames, including prestressed one and non-prestressed one, are tested and analyzed (Xue, 2011). The results reveal that both the HPC frames behave in a ductile manner and exhibit good seismic performance.

As a part of the research program and the extension of the previous studies, a four-story two-bay HPC frame is tested and analyzed in this paper in order to investigate the seismic performance of multi-story multi-bay HPC frame and the feasibility of HPC frame constructed in earthquake zone. The seismic performance in terms of failure pattern, failure mechanism, deformation restoring capacity, displacement ductility, energy dissipation capacity of the HPC frame and design principle of frame structures to ensure that the beam sidesway mechanism occurs are discussed.

2. Experimental Program

2.1 Test Specimen

A four-story two-bay HPC frame was tested under low reversed cyclic loading. The frame was designed according to the Code for seismic design of buildings (GB 50011-2010) (Ministry of Housing and Urban-Rural Development, 2010), and checked by IBC 2006 (International Code Council Inc, 2006). The frame

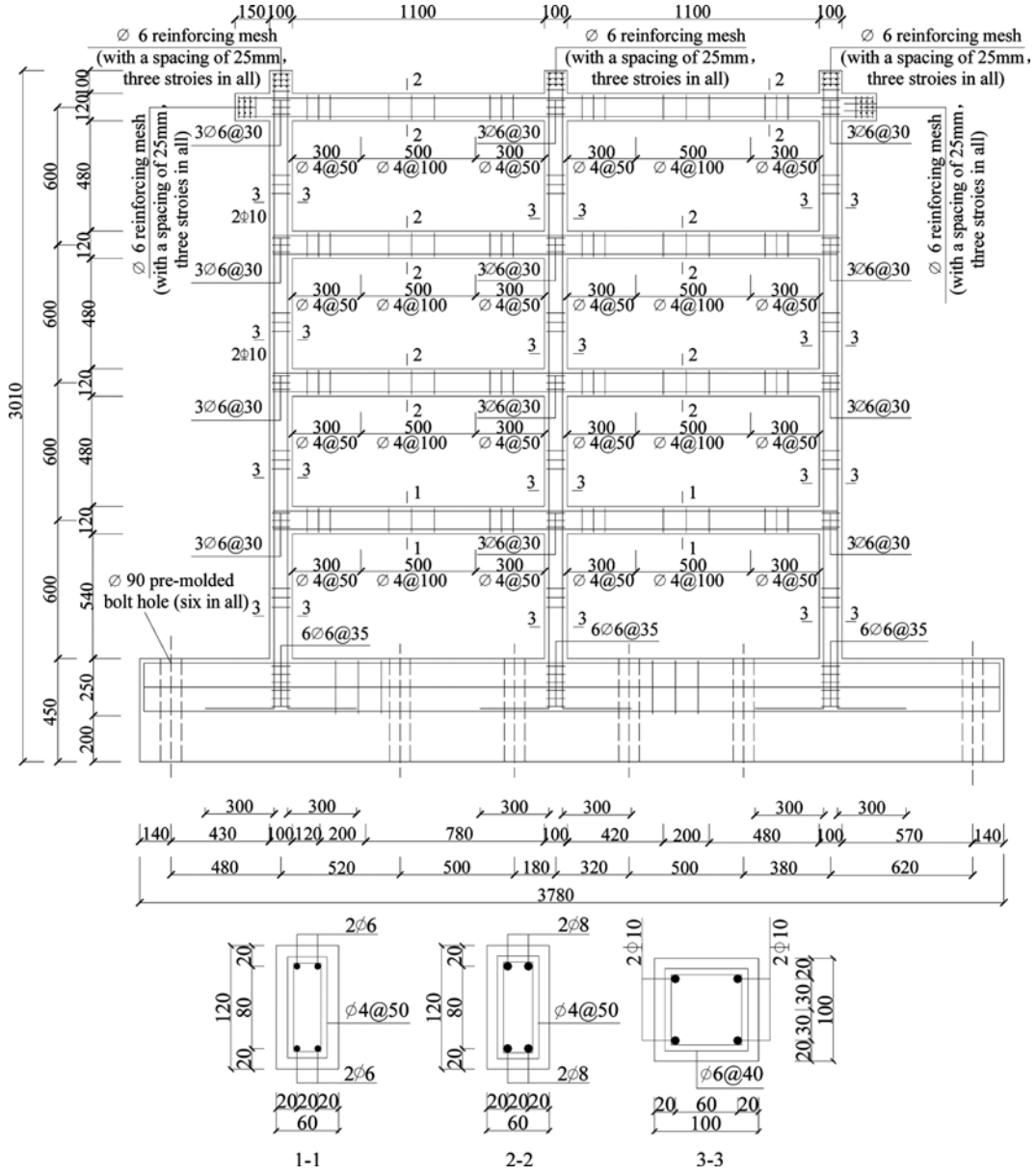

Fig. 1. Details of the Frame Specimen

Table 1. Concrete Mixture Proportion

Meterials	Quantity kg·m^{-3}
Cement	127
Grinded slag	127
Water	92
Fine aggregate	334
Coarse aggregate	500
Water reducing agent	1.3~3.8
Polypropylene fiber	0.9

Table 2. Mechanical Properties of Steel Bars

Bars Type	ϕ6	ϕ8	ϕ10
Yield strength f_y, MPa	389.2	338.6	400.5
Ultimate strength f_u, MPa	513.9	553.3	532.0
Young's modulus E_s, GPa	212	190	179
Elongation at fracture	22%	18.7%	19.3%

Table 3. Mechanical Properties of Concrete

Cylinder strength f_c', MPa	48.23
Cube strength f_{cu}, MPa	63.46
Elastic modulus E_c, GPa	39.8

specimen was a 1/5-scaled model, with the height of 0.6m for each story, right and left spans of 1.2 m. The width and depth of the beams were 60 mm and 120 mm, respectively. The cross section dimension of the columns was 100 mm by 100 mm. Details of the frame specimen are shown in Fig. 1. Note that, in order to improve the ductility supply and dissipation capacity, the frame was designed according to the proposed design principle presented in the section "Discussion of Failure Mechanisms and Design Principle" in this paper.

The mixture property of the HPC (listed in Table 1) is similar to that of HPC used in beams and two-story two-bay frames in the authors' previous studies (Xue, 2008; Xue, 2011). The maximum size of aggregate used in the test specimen frame is 15 mm. The diameters of longitudinal reinforcements in beams are 6 mm (1st floor) and 8 mm (2nd, 3rd & 4th floor), respectively, and the diameters of longitudinal reinforcements in columns are 10 mm. Note, the 6 mm and 8 mm reinforcements available in China were all plain reinforcements, and widely used in the applications in China. Grinded slag with fineness of 5×10^3 cm^2/g was added to replace part of cement for strengthening the activity of admixtures. There were also polypropylene fibers added to improve early behavior of the HPC. Mechanical properties of steel bars and concrete are tabulated in Tables 2 and 3.

2.2 Test Setup and Loading Procedure

The frame was tested under constant vertical loads and low reversed cyclic lateral loads. An overview of the test setup is shown in Fig. 2. Test was carried out at the Laboratory of Building structures in Tongji University, using the Multipurpose Structure Testing System. The actuators of the Testing System were arranged to be moved freely along the guild rail based on closed-loop control, so that the P-Δ effect could be considered

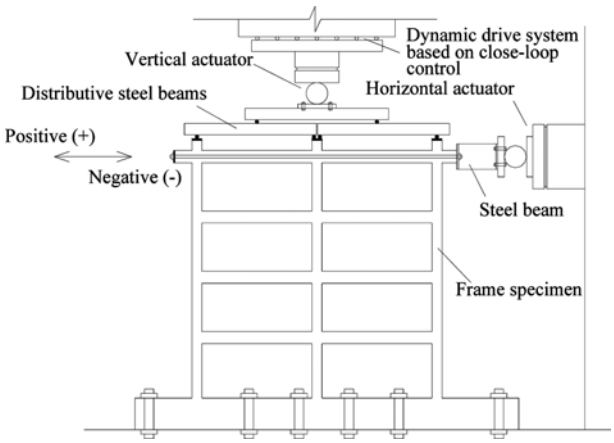

Fig. 2. Overview of the Test Setup

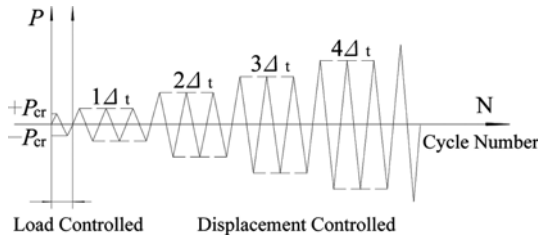

Fig. 3. Cyclic Loading History

much better. Constant vertical loads were applied to three columns by the vertical actuator of the Testing System before the lateral loads. The vertical loads applied on the interior and exterior columns were 200 kN and 100 kN, respectively. The reversed lateral loads were then applied to the top beam ends by the horizontal actuator of the Testing system with the maximum stroke of ±400 mm.

The loading history as presented in Fig. 3 was divided into two phases. The first phase was a load-controlled cycle used to determinate the cracking load. The second phase was a displacement-controlled phase, in which the frame was displaced to 16 mm for the first cycle and Δ_t = 16 mm (Roof drift = 1/150) for the remaining cycles. In the first displacement amplitude, the frame specimen was yielding. The displacement cycles consisted of $\pm1\Delta_t$, $\pm2\Delta_t$, and $\pm3\Delta_t$, etc. Three cycles were applied at each of these displacement amplitudes. In this study, the roof drift was defined as: $D_r = \Delta/H$, where H was the total height of the structure measured from the fixed column end in the first story and Δ was the lateral roof displacement of the structure.

Strain gauges were used to monitor the section strains of the concrete and longitudinal reinforcements at the beam and column ends, and of the transverse reinforcements at the beam-column joints. In addition, the roof and inter-story displacement were measured by displacement transducers.

3. Sequence of Failure

Flexural cracks initiated at beam ends in the first floor in $\pm1\Delta_t$, and they were developed gradually and penetrated to full depth

Fig. 4. Failure Patterns of the HPC Frame Specimen: (a) Beam Ends at the 2nd Story, (b) Base of the Middle Column, (c) Overview

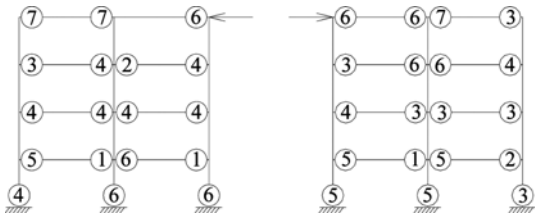

Fig. 5. Measured Developmental Sequence of Plastic Hinges

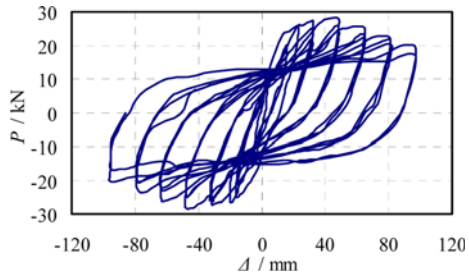

Fig. 6. Hysteresis Loops of the Applied Lateral Load (P) vs. Roof Displacement (Δ)

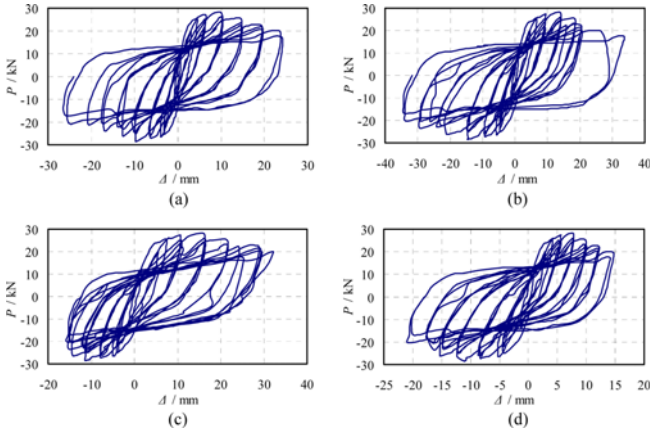

Fig. 7. Hysteresis Loops of the Applied Lateral Load (P) vs. Inter-story Displacement (Δ): (a) 1st Inter-story, (c) 3rd Inter-story, (b) 2nd Inter-story, (d) 4th Inter-story

of beam sections with the increase of displacement amplitude (Fig. 4(a)). Horizontal cracks formed at the base of the columns in the 1st displacement amplitude ($\pm 1\Delta_t$), and gradually developed in the following displacement amplitudes. Vertical cracks at the base of the columns formed at the 4th displacement amplitude. By increasing of the amplitude of applied displacement, the vertical cracks at the base of the columns increased in number and width until the concrete spall (Fig. 4(b)). Concrete at the base of middle column crushed, after yielding of sections at nearly all the beam ends, followed by buckling of longitudinal steel bars (Fig. 4(c)). No incline cracks were observed at the beam-column joints. Note, during the whole test, no splitting crack along the reinforcement formed due to the bond slip failure, which showed that the anchorage capacity of plain bars in the frame specimen is enough.

The developmental sequence of the hinge formation was measured in the test. Fig. 5 shows the formation of the plastic hinges in detail. It showed that the beam hinges formed in nearly all the four stories except for only one beam end in the top story. The plastic hinges at the base of the columns formed after most hinges developing in the beam ends, while the development of the beam hinges basically moved up from the 1st story to top story.

4. Experimental Results and Discussion

4.1 Hysteresis Loops

The applied lateral load (P) versus roof and inter-story lateral displacement (Δ) hysteretic response of the frame specimen was used to monitor the overall behavior during the test. The hysteresis loops of lateral load vs. lateral displacement are shown in Figs. 6 and 7. It could be observed that:

1. The relationship between the lateral load and the lateral displacement, including roof and inter-story lateral displacement, was basically linear before concrete cracking. The frame specimen was still in elastic stage and there was little residual deformation observed.
2. The hysteresis loops of the HPC frame specimen became nonlinear after the concrete cracking. The slopes of the roof and inter-story hysteresis loops decreased with lateral displacement increasing.
3. The hysteresis loops became much fuller and fatter in the displacement-controlled phase, accompanied by gradual stiffness degradation.
4. After the hysteresis loops reaching the maximum load point, the peak load at each level of displacement amplitude gradually decreased, but the areas of the hysteresis loops still

increased obviously, indicating the ductile behavior of reinforcements and HPC material, as well as better energy dissipation of the frame specimen.

5. Due to the cumulative damage, the strength degradation of the frame specimen could be observed via the hysteresis loops, and the maximum load of the first cycle was larger than that of the next two cycles in the same displacement amplitude.
6. The maximum displacement of the 1st and 2nd inter-story was similar at each level of displacement amplitude, and it was a little larger than that of the 3rd and 4th inter-story. The results of this situation occurred mainly because the beam hinges firstly formed at the lower stories.

4.2 Displacement Ductility and Deformability

Displacement ductility coefficient is defined as $\mu = \Delta_{ult}/\Delta_y$, which is the one of most important indices to evaluate the seismic performance of structures. Here, Δ_y and Δ_{ult} are the yield displacement and ultimate displacement of roof and different inter-story, respectively. The yield displacement Δ_y is determined according to the criteria for equivalent elasto-plastic energy absorption used by Park (Park, 1989). When the load is more than 85% of the peak load at the end of the test, the final load is as the ultimate load and the corresponding displacement is as the ultimate displacement Δ_{ult}; when the final load is less than 85% of the peak load, the ultimate displacement Δ_{ult} is determined corresponding to a 15% drop of the peak load. The displacement ductility coefficients and residual deformation ratios of the frame specimen during test are listed in Table 4. The following conclusions could be concluded:

1. The roof and inter-story ductility coefficients ranged from 4.69 to 7.95, indicating that the HPC frame specimen exhibited better ductility.
2. The ductility coefficients decreased from the bottom story to top story, because the hinges firstly formed at the beam ends in the lower stories and developed from bottom story to top story, which caused further development of the plasticity in lower stories.
3. The ratios Δ_{ult}/H of the roof, 1st inter-story, 2nd inter-story, 3rd inter-story and 4th inter-story were about 1/24, 1/25, 1/18, 1/29 and 1/35, indicating the frame specimen exhibited good deformability.

Table 4. Deformation and Ductility Coefficients of the HPC frame Specimen

Parameter		Δ_y / H	Δ_{max} / H	Δ_{ult} / H	Δ_{ult} / Δ_y	
Roof	Pos.	1/148	1/48	1/24	5.87	5.96
	Neg.	1/152	1/52	1/24	6.06	
1st inter-story	Pos.	1/194	1/59	1/26	7.51	7.95
	Neg.	1/197	1/61	1/24	8.38	
2nd inter-story	Pos.	1/129	1/42	1/18	7.06	7.32
	Neg.	1/135	1/42	1/18	7.58	
3rd inter-story	Pos.	1/113	1/37	1/19	6.07	5.06
	Neg.	1/155	1/52	1/38	4.04	
4th inter-story	Pos.	1/195	1/77	1/42	4.65	4.69
	Neg.	1/136	1/54	1/29	4.73	

4.3 Deformation Restoring Capacity

The residual displacement ratio, which is defined as $R = \Delta_r/\Delta_m$, is used as a key index to evaluate the deformation restoring capacity of structures, which decides the retrofit strategies for structures. Here, Δ_r is the roof and inter-story residual displacement after unloading, and Δ_m is equal to the maximum roof and inter-story displacement for each level of displacement amplitude. The residual deformation and residual deformation ratios of the specimen are listed in Table 5. The followings could be drawn:

1. As the cumulative damage was developed with the displacement amplitude increasing, both roof and inter-story residual deformations increased obviously, e.g. the roof residual deformation ratio increased from 0.482 (in $\pm 1\Delta_t$) to 0.908 (in $\pm 6\Delta_t$), and that of 2nd inter-story increased from 0.478 (in $\pm 1\Delta_t$) to 0.909 (in $\pm 6\Delta_t$).
2. The frame specimen was a symmetric structure, so the residual deformation ratios of roof and different inter-story in positive and negative directions were quite approximate.
3. The residual deformation ratios of roof and inter-story were quite approximate to each other at the same displacement amplitude, indicating the resistant behavior of each inter-

Table 5. Residual Displacement Ratio of the HPC frame Specimen

Displacement amplitude	2Δt		3Δt		4Δt		5Δt		6Δt	
	Pos.	Neg.	Pos.	Neg.	Pos.	Neg.	Pos.	Neg.	Pos.	Neg.
Roof	0.509	0.454	0.604	0.560	0.744	0.720	0.852	0.853	0.912	0.904
	0.482		0.582		0.732		0.853		0.908	
1st inter-story	0.462	0.431	0.566	0.546	0.743	0.818	0.855	0.861	0.938	0.921
	0.447		0.556		0.781		0.858		0.930	
2nd inter-story	0.487	0.469	0.578	0.543	0.683	0.732	0.819	0.931	0.896	0.924
	0.478		0.561		0.708		0.875		0.909	
3rd inter-story	0.569	0.400	0.690	0.487	0.830	0.582	0.875	0.623	0.910	0.829
	0.485		0.589		0.706		0.749		0.870	
4th inter-story	0.425	0.499	0.510	0.592	0.700	0.722	0.801	0.824	0.867	0.891
	0.462		0.551		0.711		0.813		0.879	

story was close.

4.4 Restoring-force Model

According to analysis of hysteresis loops of the frame specimen, a restoring-force model of the HPC frame is proposed, as shown in Fig. 8. Here, P_{cr}, P_y, P_{max}, P_{ult} stand for lateral load when frame is at the stage of cracking, yielding, ultimate load-carrying capacity and ultimate failure, respectively, and Δ_{cr}, Δ_y, Δ_{max}, Δ_{ult} are lateral displacement at these corresponding stages. In Fig. 8, "+" and "–" at the top right corner of letters denoted the characteristic values in positive and negative directions, respectively. The hysteretic rules of the proposed model were described as following:

1. The envelope of the frame specimen was simplified into four-fold line in both positive and negative directions. The characteristic points were cracking point, yielding point and peak point.
2. Frame was assumed to be in elastic range before cracking. The initial stiffness K_1 ($K_1 = P_{cr}/\Delta_{cr}$) was taken as the loading stiffness, and stiffness degradation and residual deformation were not taken into account during unloading, and reloading rules in negative direction.
3. From cracking to yielding, defined loading stiffness as yielding stiffness K_2 ($K_2 = (P_y - P_{cr})/(\Delta_y - \Delta_{cr})$), and the unloading path pointed to cracking point in the negative direction of loading. Stiffness degradation and residual deformation were considered at this stage.
4. Defined loading stiffness as the post-yielding stiffness K_3 ($K_3 = (P_{max}-P_y)/(\Delta_{max}-\Delta_y)$) after yield point and loading stiffness as negative stiffness after peak load point.
5. The initial stiffness, K_1, was assumed as the unloading stiffness by reduction factor β. Here, $\beta = (\Delta_y/\Delta_m)v$, where Δ_y was the displacement at yield point, Δ_m was the maximum displacement and v was a regressed factor from the test results.
6. After post-yield unloading in the positive direction, the reloading path in the negative direction might have two alternative directions. When the previous maximum displacement in the negative direction of loading did not exceed the cracking displacement, the reloading path directly pointed to the cracking point in the negative direction of loading. When the previous maximum displacement in the negative direction of loading exceeded the cracking displacement in negative direction, the reloading path pointed to the maximum displacement point in the negative direction of loading.
7. The frame failed when load-carrying capacity declined to 85% of its peak load or reached the ultimate deformation Δ_{ult} of the restoring-force model.

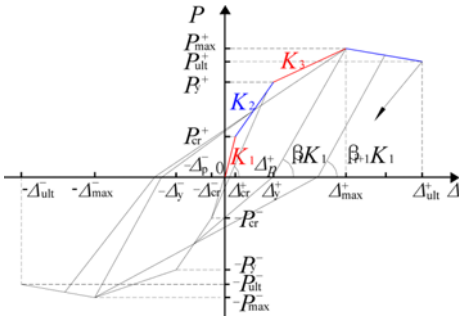

Fig. 8. Restoring-force Model of HPC Frame

According to the test results, normalized characteristic parameters of restoring-force model for the four-story two-bay HPC frame are presented in Table 6. The restoring-force model could be used for elasto-plastic analyzing and FEA of HPC frames.

4.5 Energy Dissipation

The ability of a structure to survive an earthquake depends to a large extent on its ability to dissipate the input energy. The good energy dissipation capacity indicates the capacity of the structure to perform satisfactorily in the inelastic range. A desirable behavior for a frame structure under cyclic loading implies a sufficient amount of energy dissipation without a substantial loss

Table 6. Normalized Characteristic Parameters for Hysteretic Model

Characteristic parameters		Roof		1st inter-story		2nd inter-story		3rd inter-story		4th inter-story	
		Pos.	Neg.	Pos.	Neg.	Pos.	Neg.	Pos.	Neg.	Pos.	Neg.
P_{max}		1.00	1.00	1.00	1.00	1.00	1.00	1.00	1.00	1.00	1.00
P_y		0.88	0.908	0.88	0.91	0.88	0.91	0.88	0.91	0.88	0.91
P_{cr}		0.38	0.46	0.38	0.46	0.44	0.50	0.46	0.51	0.48	0.53
P_{ult}		0.85	0.85	0.85	0.85	0.85	0.85	0.85	0.85	0.85	0.85
Δ_{max}		1.00	1.00	1.00	1.00	1.00	1.00	1.00	1.00	1.00	1.00
Δ_y		0.34	0.35	0.31	0.31	0.33	0.31	0.33	0.34	0.40	0.40
Δ_{cr}		0.06	0.08	0.03	0.03	0.08	0.10	0.08	0.10	0.11	0.12
Δ_{ult}		1.97	2.15	2.30	2.58	2.33	2.34	1.99	1.36	1.84	1.88
ν	$2\Delta_t$	1.22	1.69	1.48	1.5	1.15	1.29	1.10	1.75	1.66	1.42
	$3\Delta_t$	1.45	1.14	1.07	1.19	0.68	1.17	0.50	1.29	0.83	1.00
	$4\Delta_t$	0.78	1.03	0.77	0.79	0.80	0.88	0.66	0.82	0.81	0.73
	$5\Delta_t$	0.39	0.61	0.48	0.24	0.71	0.6	0.30	0.73	0.48	0.53
	$6\Delta_t$	0.38	0.38	0.21	0.43	0.48	0.34	0.21	0.59	0.50	0.21

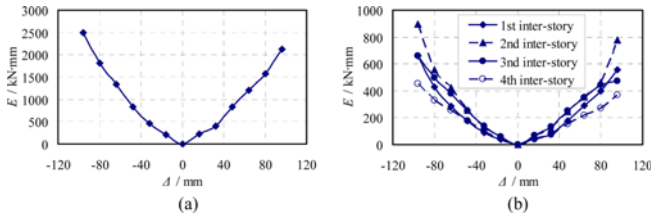

Fig. 9. Energy Dissipation Curves of the HPC frame Specimen: (a) Roof, (b) Inter-story

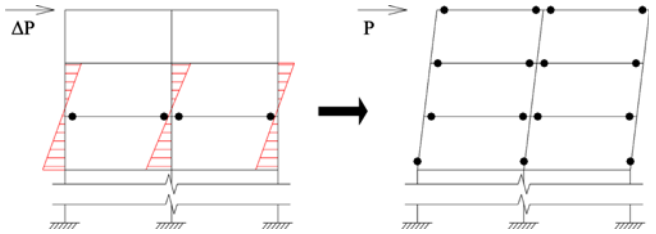

Fig. 10. Failure Mechanism with Plastic Hinges Shifting in Columns

of strength and stiffness. In this paper, the energy dissipated in a load cycle is calculated using the Trapezoid Rule to determine the area within the applied lateral load (P) versus lateral displacement (Δ) curves (Xue, 2011). The amount of energy dissipated in the frame specimen is depicted in Fig. 9. The characteristics of energy dissipation were as below:

1. The pattern of energy dissipation was almost identical between the roof and the inter-story, as the roof displacement amplitude increased, the energy dissipation capacity kept on increasing.
2. The amount of energy dissipated was very little during the first cycle, only about 10% of that at the $6\Delta_t$ for the roof and the inter-story, showing that the amount of energy dissipated at early stage was little.
3. During the elasto-plastic stage, the lateral load increased slowly and even decreased because of accumulated damage, but the energy dissipation capacity of the frame specimen still increased obviously, indicating ductile behavior of reinforcements and HPC material, as well as good energy dissipation of the frame specimen.
4. Under the same displacement amplitude, energy dissipation in the next two cycles was lower than that in the first cycle, which illustrated that damage of the frame had kept on cumulating and energy dissipation capacity degraded gradually under cyclic loading.

5. Discussion of Failure Mechanisms and Design Principle

5.1 Failure Mechanisms

Nowadays, failure mechanism control is universally recognized as one of the primary goals of structural design process (Paulay and Priestley, 1995). Studies show that the ductility supply and energy dissipation capacity of the frame structures are maximized when the beam sidesway mechanism is developed, because all the dissipative zone in the beams are involved in the corresponding pattern of yielding (Paulay and Priestley, 1995; Park and Paulay, 1975; Mazzolani and Piluso, 1995). Herein, the beam sidesway mechanism could be described as that yielding has commenced at the critical sections of the beams and developed in all the beams before the base of the columns reach yield curvature, while the other columns could remain elastic (Park and Paulay, 1975).

Nevertheless, it is difficult to guarantee the frame structures fail in beam sidesway mechanism in the practical projects. Since the plastic hinges firstly form in first story beams when the frames are subjected to the horizontal force, the development of plastic hinges tends to move up the frame in waves involving a few stories at a time (Park and Paulay, 1975). In this condition, the points of contraflexure of the story columns are much higher away from the bottom sections (see Fig. 10). As a result, the plastic hinges would more easily form at the bottom sections of the story columns, and the mixed failure mechanism instead of the beam sidesway mechanism would develop (see Fig. 10).

5.2 Design Principle and Validation

An alternative design principle of frame structures is proposed to ensure that the beam sidesway mechanism occurs. According to the proposed design principle, the development of beam hinges is required to continuously move up from the 1st story to top story, and then the plastic hinges form at the base of columns. In this pattern of yielding, the failure mechanism shown in Fig. 10 could be effectively avoided. In order to demonstrate that the ductility supply of the frame designed according to the proposed design principle is maximized, parametric analysis of ten frames with different development of hinges is conducted. An open source object-oriented software framework for finite element analysis OpenSees (Open System for Earthquake Engineering Simulation) is used for the parametric analysis, and the FE model is validated firstly by the test results of the frame specimen in this paper.

OpenSees was developed at the University of California, Berkeley, primarily to support earthquake simulations (Mckenna, 2008). The frame structures are commonly modeled using the non-linear beam-column element in OpenSees. Fiber sections are integrated along the members of the frame models using the Gauss-Labotto integration scheme. These sections consist of steel, confined concrete and unconfined concrete uniaxial material models. The steel material model is a basic model that incorporates isotropic strain hardening, while the concrete material model represents the concrete crushing and residual strength in compression and tensile strength with linear strain softening (Taucer *et al.,* 1991; Scott *et al.,* 1982). Note that, the characteristic parameters of concrete material model using in the FEA in this paper were obtained from the test results in the previous studies (Cheng, 2003).

Hysteresis performance of the frame specimen was analyzed using OpenSees. Fig. 11 shows the test and analytical loops of

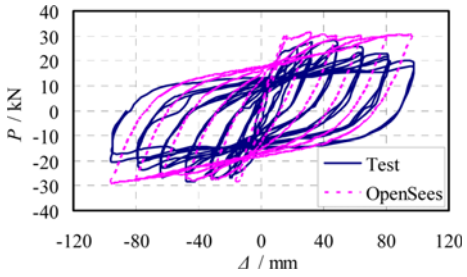

Fig. 11. Test and Analytical Hysteresis Loops

lateral load vs. roof lateral displacement. It can be observed that the beginning of the test up to the failure of the frame specimen, the test and analytical results were generally in good agreement, although the strength degradation was not caught very well. It is indicated the analytical model based on OpenSees can provide a good simulation for the full-range hysteresis analysis of frame structures.

There were ten four-story two-bay frames were designed according to the specified failure mechanisms. As listed in Table 7, the frames were divided into four sets (i.e., SL1, SL2, SL3 and SL4) and named as SL*i*-*j*, in which the italics *i* and *j* stood for that the development of beam hinges were designed to move up from the *i*th story to *j*th story. For example, SL1-3 stood for that the development of beam hinges were designed to move up from the 1st story to 3rd story. The longitudinal reinforcements in different story beams are optimized to ensure the frames fail in the designed hinge formations which are list in the Table 7. The beam-column joints of the frames are sufficient strengthened to prevent the joints fail prior to the beams and columns. Note that, SL1-4 was designed according to the proposed design principle.

The analytical curves of the normalized applied lateral load (P/P_u) versus roof lateral displacement (Δ) are shown in Fig. 12, while the lateral load was applied on the roof. Herein, failure of the ten frames is determined according to two criterions, one is defined by the OpenSees, and the other is suggested by Park (Park, 1989). In the Opensees, when the concrete at the hinges crushed, the FEA terminated because of non-convergence, and the frames are assumed as failed. In the criterion suggested by Park, the frames are assumed as failed when the final load is less

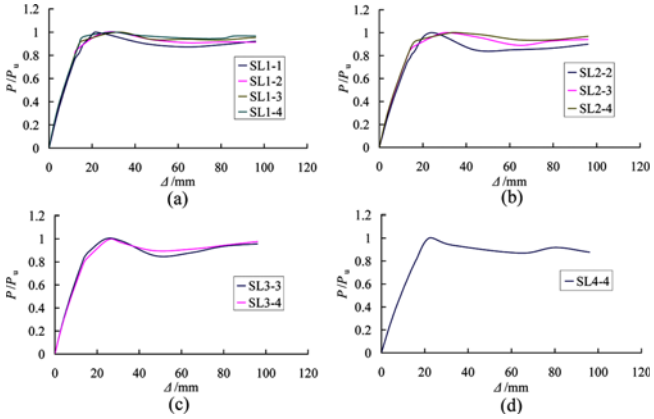

Fig. 12. P/P_u Vs. Δ Curves of the Frames: (a) Set SL1, (b) Set SL2, (c) Set SL3, (d) Set SL4

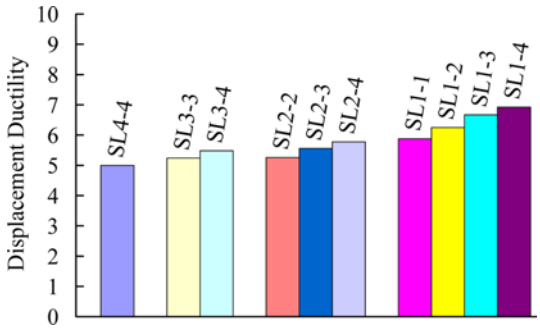

Fig. 13. Displacement Ductility Coefficients of the Frames

than 85% of the peak load. The ultimate lateral load P_{ult} of the ten frames should take the greater one according to the two criterions.

The roof displacement ductility coefficients *m* of the ten frames are depicted in Fig. 13. The followings could be concluded:

1. The development of beam hinges for SL1-4 moved up from the 1st story to top story, and the frame finally failed in beam sidesway mechanism. It shows that the proposed design principle could sufficiently ensure that the beam sidesway occurs. The displacement ductility of SL1-4 was 6.92, and it was the best one among the ten frames.
2. The displacement ductility coefficients of the SL1-1, SL1-2, SL1-3 and SL1-4 were about 5.88, 6.25, 6.67 and 6.92. The

Table 7. Development of Plastic Hinges of the Frames

Specimens		Development of plastic hinges
Set SL1	SL1-1	1st story beam ends → column ends
	SL1-2	1st story beam ends → 2nd story beam ends → column ends
	SL1-3	1st story beam ends →2nd story beam ends → 3rd story beam ends → column ends
	SL1-4	1st story beam ends → 2nd story beam ends → 3rd story beam ends → 4th floor beam ends → column ends
Set SL2	SL2-2	2nd story beam ends → column ends
	SL2-3	2nd story beam ends → 3rd story beam ends → column ends
	SL2-4	2nd story beam ends → 3rd story beam ends → 4th floor beam ends → column ends
Set SL3	SL3-3	3rd story beam ends → column ends
	SL3-4	3rd story beam ends → 4th floor beam ends → column ends
Set SL4	SL4-4	4th floor beam ends → column ends

corresponding values of SL2-2, SL2-3 and SL2-4 were about 5.26, 5.56 and 5.78. While the values of SL3-3 and SL3-4 was about 5.24 and 5.48. It shows that the ductility of the frame structures is improved with the magnitude of the beam hinges increasing.

3. As listed in Table 7, all the beam hinges of SL1-1, SL2-2, SL3-3 and SL4-4 formed in only one story, that's the 1st story, the 2nd story, the 3rd story and the top story, respectively. The displacement ductility coefficients of the frames were about 5.88, 5.26, 5.24 and 5.00. All the beam hinges of SL1-2, SL2-3 and SL3-4 formed in two stories, those are the 1st & 2nd stories, 2nd & 3rd stories and 3rd & 4th stories respectively. The displacement ductility coefficients of the frames were about 6.25, 5.56 and 5.48. It is concluded that when the magnitude of beam hinges is the same, the ductility of the frame that the beam hinges firstly form in the lower story is better than that firstly form in the upper story.

6. Conclusions

Based on the cyclic loading test of the 1/5-scaled HPC frame specimen and the discussion of failure mechanisms and design principle, the following conclusions can be drawn from the study:

1. The HPC frame specimen was failed due to the concrete at base of middle columns crushed after yielding of the sections at beam ends, followed by buckling of longitudinal steel bars. The frame specimen basically fails in beam sidesway mechanism with the development of beam hinges moving up from the 1st story to top story, which provides good ductility supply and energy dissipation capacity. The design intention was achieved.
2. The HPC frame specimen exhibited a stable lateral load versus drift hysteretic response. The areas of all the roof and inter-story hysteretic loops became larger with increasing drift, even in the loading stage that the peak load at each level of displacement amplitude gradually decreased. The reason lied in the ductile behavior of reinforcements and HPC material, as well as better energy dissipation of the frame specimen.
3. The roof lateral displacement ductility coefficient was 5.69, and the 1st, 2nd, 3rd and 4th inter-story lateral displacement ductility coefficients were 7.95, 7.32, 5.06 and 4.69 respectively. These results indicated that the HPC frame behaved in a ductile manner. The ductility coefficients decreased from the bottom story to top story, because the hinges firstly formed at the beam ends in the lower stories and developed from bottom story to top story, which caused further development of the plasticity in lower stories.
4. An alternative design principle of frame structures is proposed to ensure that the beam sidesway mechanism occurs. According to the design principle, the development of beam hinges is required to continuously move up from the 1st story to top story, and then the plastic hinges form at the base of columns. Parametric analysis of ten frames with different development of beam hinges is conducted by using OpenSees. The results show that the ductility supply of the frame designed according to the proposed design principle is maximized.

Acknowledgements

This study was financially supported by the National Natural Science Foundation of China (No. 51508400) and the Science and Technology Commission of Shanghai Municipality (15DZ1203502).

References

Alameddine, F. and Ehsani, M. R. (1991). "High-strength RC connections subjected to inelastic cyclic loading." *Journal of Structural Engineering,* Vol. 117, No. 3, pp. 829-850, DOI: 10.1061/(ASCE)0733-9445 (1991)117:3(829).

Anderson, J. C., Duan, X., Yin, Z., and Mansouri, B. (1997). "Cyclic behaviour of high strength concrete joints." *Structures Congress-Proceedings, Building to Last*, Vol. 1.

Ashitiani, M. S., Dhakal, R. P., and Scott, A. N. (2014). "Seismic performance of high-strength self-compacting concrete in reinforced concrete beam-column joints." *Journal of Structural Engineering*, Vol. 140, No. 5, pp. 1-12, DOI: 10.1061/(ASCE) ST.1943-541X. 0000973.

Awati, M. and Khadiranaikar, R. B. (2012). "Behavior of concentrically loaded high performance concrete tied columns." *Engineering Structures*, Vol. 37, No. 4, pp. 76-87, DOI: 10.1016/j.engstruct. 2011.12.040.

Breitenbücher, R. (1998). "Developments and applications of high-performance concrete." *Materials & Structures*, Vol. 31, No. 3, pp. 209-215, DOI: 10.1007/BF02480402.

Biolzi, L., Cattaneo, S., and Mola, F. (2014). "Bending-shear response of self-consolidating and high-performance reinforced concrete beams." *Engineering Structures*, Vol. 59, No. 2, pp. 399-410, DOI: 10.1016/j.engstruct.2013.10.043.

Cheng, B. (2003). "Study on seismic performance and performance-based design of HPC frames. Master's thesis." *Department of Building Engineering.* Tongji Univ. Shanghai, China. (Supervised by W. C. Xue)

Fang, I. K., Wang, C. S., and Hong, K. L. (1994). "Cyclic behaviour of high-strength concrete short beams with low amout of flexural reinforcement." *ACI Structural Journa*l, Vol. 91, No. 1, pp. 10-18, DOI: 10.14359/4477.

International Code Council Inc. (2006). "International Building Code IBC 2006." Country Club Hill, IL.

Lin, C. H. and Lee, F. S. (2001). "Ductility of high-performance concrete beams with high-strength lateral reinforcement." *ACI Structural Journal*, Vol. 98, No. 4, pp. 600-608. DOI: 10.14359/10303.

Ministry of Housing and Urban-Rural Development (2010). "Code for Seismic Design of Buildings GB50010-2010." Beijing, China.

Mazzolani, F. M. and Piluso, V. (1995). "Failure mode and ductility control of seismic resistant MR-frames." *Costruzioni Metalliche*, Vol. 2, pp. 11-28.

McKenna, F., Fenves, G. L., and Scott, M. H. (2008). "Open system for earthquake engineering simulation." *Pacific Earthquake Engineering Research Center*, University of California at Berkeley, California.

Neville A. and Aitcin P. C. (1998). "High performance concrete-an

overview." *Materials & Structures*, Vol. 31, pp. 111-117, DOI: 10.1007/BF02486473.

Prasad, K. R., Bharatkumar, B. H., Ramachandra, D. S., Narayanan, R., and Gopalakrishnan, S. (2005). "Fracture mechanics model for analysis of plain and reinforced high-performance concrete beams." *Journal of Engineering Mechanics*, Vol. 131, No. 8, pp. 831-838, DOI: 10.1061/(ASCE)0733-9399(2005)131:8(831).

Priestley, V. J. N., Verma, R., and Xiao, Y. (1994). "Seismic shear strength of reinforced concrete columns." *Journal of Structural Engineering*, Vol. 120, No. 7, pp. 2310-2329, DOI: 10.1061/(ASCE) 0733-9445(1994)120:8(2310).

Park, R. (1989). "Evaluation of ductility of structures and structural assemblages from laboratory testing." *Bulletin of the New Zealand National Society for Earthquake Engineering*, Vol. 22, No. 3, pp. 155-166.

Paulay, T. and Priestley, M. J. N. (1995). *Seismic design of reinforced concrete and masonry buildings*, John Wiley & Sons. Ltd. New York.

Park, R. and Paulay, T. (1975). *Reinforced Concrete Structures*, John Wiley & Sons. Ltd. New York.

Scott, B. D., Park, R., and Priestley, M. J. N. (1982). "Stress-strain behavior of concrete confined by overlapping hoops at low and high strain rates." *ACI Journal*, Vol. 84, No. 4, pp. 13-27, DOI: 10.14359/ 10875.

Taucer, F. F., Spacone, E., and Filippou, F. C. (1991). *A Fiber Beam-column Element for Seismic Response Analysis of RC Structures EERC Report 91/17*, Earthquake Engineering Research Center. University of California. Berkeley. CA.

Woods, J. M., Kiousis, P. D., Ehsani, M. R., Saadatmanesh, H., and Fritz, W. (2007). "Bending ductility of rectangular high strength concrete columns." *Engineering Structures*, Vol. 29, No. 8, pp. 1783-1790, DOI: 10.1016/j.engstruct.2006.09.024.

Wu, K. R., Yan, A., Yao, W., and Dong Z. (2001). "Effect of metallic aggregate on strength and fracture properties of HPC." *Cement & Concrete Research*, Vol. 31, No. 2, pp. 113-118, DOI: 10.1016/ S0008-8846(00)00431-2.

Xiao, Y. and Ma, R. (1998). *Seismic Behaviour of High Strength Concrete Beams*, John Wiley & Sons. Ltd. Structural design tall building.

Xiao, Y. and Martirossyan, A. (1998). "Seismic performance of high-strength concrete columns." *Journal of Structural Engineering*, Vol. 124, No. 3, pp. 241-251, DOI: 10.1061/(ASCE)0733-9445 (1998)124:3(241).

Xue, W. C., Li, L., Cheng, B., and Li, J. (2008). "The reversed cyclic load tests of normal and pre-stressed concrete beams." *Engineering Structures*, Vol. 30, pp. 1014-1023, DOI: 10.1016/j.engstruct.2007. 06.001.

Xue, W. C., Cheng, B., and Li, L. (2011). "Seismic performance of nonprestressed and prestressed HPC frames under low reversed cyclic loading." *Journal of Structural Engineering*, Vol. 137, No. 11, pp. 1254-1262, DOI: 10.1061/(ASCE)ST.1943-541X.0000367.

Yao, W., Li, J., and Wu, K. R. (2003). "Mechanical properties of fiber-reinforced concrete at low fiber volume fraction." *Cement & Concrete Research*, Vol. 33, No. 1, pp. 27-30, DOI: 10.1016/ S0008-8846(02)00913-4.